FEMS Microbiology Ecology, 2023, **99**, 1–12
DOI: 10.1093/femsec/fiad146
Advance access publication date: 21 November 2023
Research Article

Impact of dilution on stochastically driven methanogenic microbial communities of hypersaline anoxic sediments

Francisca Font-Verdera[1,*,‡], Raquel Liébana[1,2,‡], Ramon Rossello-Mora[1,*], Tomeu Viver[1,3]

[1]Mediterranean Institute for Advanced Studies (IMEDEA, UIB-CSIC), Miquel Marquès, 21, 07190 Esporles, Illes Balears, SPAIN
[2]AZTI, Basque Research Technology Alliance (BRTA), Txatxarramendi ugartea z/g, Sukarrieta, 48395 Sukarrieta, Bizkaia, Spain
[3]Max Planck Institute for Marine Microbiology, Celsiusstraße 1, 28359 Bremen, Germany
*Corresponding authors. Mediterranean Institute for Advanced Studies (IMEDEA, UIB-CSIC); Miquel Marquès, 21; 07190 Esporles; Illes Balears Spain. Tel: +34 971 61 18 18; Fax: +34 971 61 17 61; E-mails: xfont@imedea.uib-csic.es; ramon@imedea.uib-csic.es
‡Both authors contributed equally to the manuscript.
Editor: [Tillmann Lueders]

Abstract

Sediments underlying the solar salterns of S'Avall are anoxic hypersaline ecosystems dominated by anaerobic prokaryotes, and with the especial relevance of putative methanogenic archaea. Slurries from salt-saturated sediments, diluted in a gradient of salinity and incubated for > 4 years revealed that salt concentration was the major selection force that deterministically structured microbial communities. The dominant archaea in the original communities showed a decrease in alpha diversity with dilution accompanied by the increase of bacterial alpha diversity, being highest at 5% salts. Correspondingly, methanogens decreased and in turn sulfate reducers increased with decreasing salt concentrations. Methanogens especially dominated at 25%. Different concentrations of litter of *Posidonia oceanica* seagrass added as a carbon substrate, did not promote any clear relevant effect. However, the addition of ampicillin as selection pressure exerted important effects on the assemblage probably due to the removal of competitors or enhancers. The amended antibiotic enhanced methanogenesis in the concentrations ≤ 15% of salts, whereas it was depleted at salinities ≥ 20% revealing key roles of ampicillin-sensitive bacteria.

Keywords: 16S rRNA gene; ampicillin; anaerobic hypersaline sediments; methane; microcosms; salinity

Introduction

Environmental factors such as pH, alkalinity, (total) carbon availability, UV irradiation, ionic composition, and especially salinity, have been largely evaluated for their influence on microbial communities (Walsh et al. 2005, Lozupone and Knight 2007, Swan et al. 2010, Sierocinski et al. 2018, Viver et al. 2020). In this regard, salinity has been described as the major environmental factor driving microbial community assembly in a wide range of environments (Lozupone and Knight 2007). The microbial selective forces applied by salinity have been studied in numerous habitats with temporal or spatial salinity gradients, such as estuaries, wetlands, salt marshes, and coastal lagoons (Walsh et al. 2005, Swan et al. 2010, Webster et al. 2015, Xie et al. 2017). In natural ecosystems where salinity gradients exist, the abundance and activity of prokaryotic communities are high, due to the amount of available electron acceptors and donors, nutrients, and carbon sources (McGenity and Sorokin 2019). Oxygen-free environments harbor a great richness of anaerobic microorganisms related to carbohydrate synthesis and degradation, fermentation of polysaccharides, sulfate- and nitrate-dissimilatory reduction, and methanogenesis (Gottschalk 1979), for which the high salinities of hypersaline sites are not an obstacle (McGenity and Sorokin 2019). Therefore, a relevant potential for methanogenesis has been recently discovered in hypersaline environments that should be further described. Moreover, salinity acts as a metabolic modulator, enhancing or impairing certain biochemical processes, thus directly affecting the biogeochemical cycles (McGenity and Oren 2012, Serrano-Silva et al. 2014, Webster et al. 2015, Zhang et al. 2017, Wang et al. 2018). Besides salinity, total organic carbon is a another studied factor that influences the structuration of the microbial communities (Salton Sea; Swan et al. 2010). In surface and subsurface saline soils, total organic carbon and pH were the primary drivers in the prokaryotic community distribution along an ecological gradient of salinity (Xie et al. 2017).

The knowledge of the drivers or forces that structure community composition is essential for understanding the ecology of microbial communities. The information obtained by alpha- and beta-diversity indices, and the development of null-model approaches, have been frequently utilized to quantify how deterministic or stochastic factors are contributing in microbial community assembly processes (Chase et al. 2011, Stegen et al. 2012, 2013, Langenheder et al. 2017, Liébana et al. 2019). It has been reported that deterministic and stochastic factors appear simultaneously but with different relative importance (Stegen et al. 2013, Dini-Andreote et al. 2015, Vass 2020). On the one hand, if stochastic processes (i.e. random birth, death, colonization, extinction, and speciation) prevail in determining microbial community composition differences among environments with similar abiotic conditions, it is expected a high variation in species composition within them. On the other hand, deterministic processes are mostly responsible of the differences among microbial communities of sites with

Received 27 April 2023; **revised** 2 October 2023; **accepted** 20 November 2023

important differences in environmental conditions (i.e. salinity and irradiation; Chase et al. 2011, Stegen et al. 2013, Zhou et al. 2014).

Solar salterns allow the study of how microorganisms physiologically and genetically adapt to high ionic concentrations, and constitute a source of microbial taxonomic novelty (Antón et al. 2000, Oren 2008, Santos et al. 2012, Gomariz et al. 2015, Mora-Ruiz et al. 2015, Martin-Cuadrado et al. 2019, Ramos-Barbero et al. 2019, Viver et al. 2019, 2020, Font-Verdera et al. 2021). In general, the aerobic brines have largely been the focus of reported studies, especially for the effect of the salinity gradient on microbial ecosystem structures and metabolic activity (McGenity and Oren 2012, Viver et al. 2019). However, hypersaline anaerobic sediments underlying these brines have been scarcely examined (e.g. López-López et al. 2010, 2013, Munoz et al. 2011, Sorokin et al. 2017a).

Extremely saline anaerobic sediments are mostly dominated by unknown taxa (López-López et al. 2010, Font-Verdera et al. 2021), but the majority of the cultivated extreme halophilic anaerobes are methanogenic members affiliating with known taxa of the *Euryarchaeota* (or recently renamed *Methanobacteriota*) phylum as of the family *Halobacteria*, which are the most retrieved in pure cultures. Also, most retrieved anaerobes are well members of the bacterial domain with either fermentative, denitrifying, or sulfate-reduction metabolisms (McGenity and Oren 2012, Font-Verdera et al. 2021, Cheng et al. 2023, Hatzenpichler et al. 2023). Representatives of diverse methanogenic metabolisms have been described especially from the archaeal domain, such as the methylotrophic *Methanohalophilus* sp. and *Methanococcoides* sp. (Lazar et al. 2011, Zhuang et al. 2016), members of the *Methanonatronarchaeia* class involved in a newly discovered methyl-reducing pathway (Sorokin et al. 2017b), and the methanogenic representatives of the *Candidatus* MSBL1 lineage (Mediterranean Sea Brine Lakes; van der Wielen et al. 2005, Yakimov et al. 2013, 2015, Font-Verdera et al. 2021).

Here, we have been working with samples from S'Avall solar salterns, located in Mallorca (Balearic Islands) that have saline concentrations close to NaCl saturation (~37%; Viver et al. 2020). We have previously shown that the oxygen-depleted sediments underlying brines in S'Avall, contain an important population of potential methanogens (López-López et al. 2010, 2013) and in especial some belonging to the candidate lineages DHVE2 and MSBL1, that seem to be especially involved in methanogenesis at high salinities (Font-Verdera et al. 2021). However, the effect of a broad salinity gradient shift on microbial diversity from these sediments has not been analyzed yet, and even less other likely important and discriminant abiotic factors, such as carbon substrate availability or the presence of inhibitors or antibiotics (Sanz et al. 1996, Jiang et al. 2007, Webster et al. 2015, Xie et al. 2017).

The current study evaluates the salt concentration in a broad salinity gradient (30%–5%) as selection force to structure the microbial communities in anoxic sediments, and also the effect on the methane production. Here, we also evaluated the effect of amending the enrichments with different concentrations of the marine angiosperm *Posidonia oceanica* leaf litter as carbon-rich substrate given that biomass of marine photosynthetic organisms has been recently proposed as substrates for methane generation (Dębowski et al. 2013, Zhang et al. 2017). Since this material is probably actively mineralized in anaerobic processes (Cocozza et al. 2011), *P. oceanica* leaf litter could also serve as carbon source for fermenters.

Finally, we have evaluated the effect of ampicillin to modulate the communities to obtain the best yielding methanogenic consortium for biotechnological purposes (Sanz et al. 1996). Previous studies have assessed the effect of this antibiotic in ecosystems such as soils, wastewater or freshwater (Ye et al. 2020), where ampicillin (which overall targets susceptible and usually Gram-positive bacteria) decreased the abundance of certain community members, hindering relevant ecosystem metabolic functions (Ferrer et al. 2017, Baumgartner et al. 2020, Ye et al. 2020). But to our knowledge, the study of antibiotic effects in hypersaline anoxic environments has never been performed.

Materials and methods

Experimental setup and samples' collection

Sediments from a basin adjacent to the crystallizer ponds of the S'Avall Mediterranean solar salterns were sampled in December 2016 using methacrylate cores to collect the top 25 cm. The features and location of this ephemeral pond were the same as previously described (Font-Verdera et al. 2021). The cores were sealed and transported to the laboratory for further processing in the following 24 h. Sediments were manipulated inside a rigid anaerobic chamber (Coy Laboratory Products Inc., USA), with controlled conditions by displacing the air using continuous N_2 flow to achieve the absence of oxygen (using a Lutron PO2-250 oxygen meter). Hydrogen was not used to remove free oxygen. Overlaying brines were discarded and all cores were pooled and homogenized by stirring the slurry. A fraction was taken (S sample) as time-zero of the experiment. A battery of sludge was prepared at eight different salinities (5%, 10%, 12%, 15%, 18%, 20%, 25%, and 30%) from the sediment slurry that contained 34.4% of salts by adjusting the concentrations mixing with seawater (4%) and brine at 25.4% of salinity. The broad range of salinity was chosen to cover the maximum range of saline concentrations that would modulate the microbial community structures with the purpose to determine the best yielding methanogenic consortium for biotechnological purposes. Seawater and brines used to dilute the sediments were both previously bubbled with N_2 for 15 h to ensure the anaerobic conditions. In addition, the slurries were amended with dry leaf casts of *P. oceanica* (*Po*) at three distinct concentrations: 0.1% w/w, 1% w/w, and 10% w/w. Finally, half of the cultures were supplemented with ampicillin (5 mg/ml). Serum bottles contained final volumes of 100 ml except for the lowest salinity (5%) with 200 ml of volume with half of the bottle space for gas production. The various permutations varying the eight salinities, the three *Po* concentrations, the antibiotic addition, and duplicates generated a total number of 96 cultures. The nomenclature for these samples was W_XYZ, where W: salinity percentage (5%, 10%, 12%, 15%, 18%, 20%, 25%, or 30%), X: *Po* percentage (0.1%, 1%, or 10%), Y: presence of ampicillin (A) or not (_), and Z: the duplicate (1 or 2). These microcosms were incubated at 30ºC during 4.5 years. For the quantification of the chemical parameters, samples were filtered through hydrophilic PTFE filters and sent to the scientific services of the University of Alicante to be chemically analyzed as indicated below (Font-Verdera et al. 2021).

Methane generation from microcosms

Methane gas (CH_4) production during the incubation of the 96 microcosms was quantified in different occasions (sampling time points can be found on the x-axis of Figure S1, Supporting Information) during 52 months (from December 2016 to March 2021) using gas chromatography. Concentrations of CH_4 were determined with a Clarus 600 gas chromatograph (Perkin Elmer, USA) equipped with a flame ionization detector (FID). The FID was used for measurements with an Elite-Plot Q packed column (Perkin Elmer, 30 m, 0.25 mm ID, 0.25 um; Crossbond 5%

diphenyl–95% dimethylpolysiloxane). Helium was used as a carrier gas at a flow rate of 5 ml/min, and oven and detector temperatures were set at 50 and 200°C, respectively. A CH_4 pure standard (≥ 99.0%, Sigma-Aldrich) was used as a reference in order to determine the retention time of the CH_4 peak. A volume of 300 μl of the headspace were injected into the gas chromatograph at 200°C with a GT 1750RN syringe for methane quantification.

Geochemical properties of cultures

Chemical parameters of all microcosms and the slurry sample were analyzed. Concentrations of anions fluoride, chloride, bromide, nitrate, and sulfate, and of cations sodium, potassium, lithium, ammonium, magnesium, and calcium were appraised by ion chromatography by Technical Research Services of Alicante University (Spain). pH was measured from previously centrifuged samples at 13 200 rpm (centrifuge 5415 R, Eppendorf) during 5 min, in two time-points, at time-zero and in July 2021 (final time) with Whatman® Panpeha™ pH indicator strips (Sigma-Aldrich). Salinity was checked by a Sper Scientific Salt Refractometer, and organic matter and carbonates were measured with the loss on ignition method (LOI) in a Muffle Furnace (Nabertherm), using the methodology reported in Font-Verdera et al. (2021).

Prokaryotic DNA extraction and 16S rRNA gene amplification

Prior to DNA extraction, 1 ml of homogenized biomass was extracted from all microcosms and time-zero sample (S). Microbial DNA extraction was performed from 0.3 to 0.4 g of mixed biomass, using the kit DNAeasy® PowerSoil® Pro Kit (Qiagen, Germany), following the manufacturer's instructions. Extracted DNA was concentrated with a SpeedVac™ system (Thermo Scientific™ SPD121P-230) and was quantified with a Qubit HS DNA kit and Qubit 4.0 Fluorimeter (Invitrogen, Thermo Fisher Scientific).

The 16S rRNA gene was amplified in all 96 cultures and the slurry (S) with the primer pair 515F (5′-GTGCCAGCMGCCGCGGTAA-3′) and 806R (5′-GGACTACHVGGGTWTCTAAT-3′; Caporaso et al. 2011), targeting the V4 region of the 16S SSU rRNA and designed to amplify both bacteria and archaea using paired-end 16S community sequencing on the Illumina platform to incorporate tags. PCR reaction mixtures and thermocycler conditions were performed as detailed by Caporaso et al. (2011), with the exception of using a DNA template of 10 μl for the reaction but acquiring a final volume of 50 μl for each sample. The bands were visualized in 1% (w/v) agarose gel electrophoresis in TAE 1X. Amplicons quality was checked with the Qubit 4.0 Fluorimeter and were sent to Macrogen Inc. (Seoul, Rep of Korea) for sequencing through Illumina Miseq™ technology. The 16S rRNA gene amplicon sequences of the 96 microcosms and the sample S (slurry) were submitted to the European Nucleotide Archive (ENA) under the study number PRJEB54035, and accession numbers from ERS12430850 to ERS12430946.

Sequence trimming and phylogenetic affiliation based on 16S rRNA amplicons

Paired-end reads from Illumina amplicon sequencing were processed with DADA2 R package (Callahan et al. 2016). The longest representative of the obtained amplicon sequence variants (ASVs) were aligned with SINA tool (Pruesse et al. 2012), and further inserted by parsimony in a Neighbor-Joining tree reconstructed with the largest and representative sequences obtained from the reported study by Font-Verdera et al. (2021). This previous phylogenetic reconstruction was performed aligning the sequences with SINA tool, inserted to nonredundant SILVA REF138 and to LTP128 (Yarza et al. 2010) databases using the ARB software package (Ludwig et al. 2004). Closest reference species in both databases were selected and a set of supporting species of high quality and covering all major phyla of archaea and bacteria were added. These were used to build the Neighbor-Joining tree with Jukes–Cantor correction. ASVs were grouped in OPUs (operational phylogenetic unit, equivalent to species; França et al. 2015) based on visual inspection of the final tree as previously published (Mora-Ruiz et al. 2015, 2016, 2018, Viver et al. 2017, Font-Verdera et al. 2021). Considering that each OPU clade generally occurs within a sequence distance of > 97% (considering that the partial sequences are only ∼400 pb) we were confident that one OPU correctly represented a single species (Mora-Ruiz et al. 2016). A metabolic inference from the phylogenetic affiliation of the OPUs, with relative sequence abundances ≥ 1%, and their putative associated and/or described metabolism was performed with the available literature.

Statistical analyses and null models

Diversity indexes, richness estimators and rarefaction curves based on OPU abundances were obtained through PAST (PAleontological STatistics) v.2.23 (Hammer et al. 2001). Alpha-diversity indices (Shannon and Dominance) have been employed to assess the local biological diversity and richness within microbial communities. These indices are useful in the quantification of species diversity (richness) within a functional community at a local scale, and subsequently, the beta-diversity (based on Bray–Curtis index) to illustrate the changes in community composition. Bray–Curtis dissimilarity was calculated in order to study the dispersion and identify the differences among samples (regarding to the ampicillin, substrate concentration and salinity), and were evaluated using principal coordinates analysis (PCoA) and nonmetric multidimensional scaling (NMDS) with the vegan package (Oksanen et al. 2018) in R v.3.6.0. (www.r-project.org). Additionally, Bray–Curtis data were also plotted employing the packages gplots and ggplot2, whilst DESeq2 was applied to discern patterns among salinities, antibiotic addition and in relation to the slurry. Permutation *D*-test, Kolmogorov–Smirnov (applying the Bonferroni correction) and *T*-test were performed to confirm the biological duplicates, and the Wilcoxon and the Mann–Whitney *U* nonparametric tests were applied in order to identify the salinity which caused the most relevant change in comparison to the original sediment (S) in R v.3.6.0. Moreover, Nonpareil curves and the logarithmic diversity index Nd were determined as coverage estimators of the community sampled with default parameters (Rodriguez-R and Konstantinidis 2014, Rodriguez-R et al. 2018).

Computational calculations based on Null Model Analysis to describe the ecology of the studied ecosystem were performed. Phylogenetic inference was estimated with ß-nearest taxon index (ßNTI), as previously described (Stegen et al. 2012, 2013, Liébana et al. 2019). Pairwise comparisons in relation to time-zero sample (S) with |ßNTI| > 2 were considered statistically relevant and indicated that communities were governed by selection. Negative or positive values of ßNTI meant that samples were more phylogenetically similar than expected by chance or more phylogenetically distant from each other, respectively. Values comprised between −2 and 2 were not significantly different from the null expectation, which point that stochastic factors influenced the phylogenetic turnover (Stegen et al. 2013). Taxonomic

turnover was estimated through the modified method of Raup–Crick metric, based on Bray–Curtis dissimilarities (RC_{bray}) as previously reported (Chase et al. 2011, Stegen et al. 2013). The RC_{bray} values ranged between −1 (two communities are more similar, than expected by chance) and 1 (two communities are more dissimilar), while a value of 0 represented no difference in the dissimilarity from the null expectation. $|RC_{bray}| < 0.95$ was not considered statistically significant and so indicator of the high influence of the stochastic factors (Chase et al. 2011, Zhou et al. 2014). Therefore, combining the two indices in the pairwise comparison, and when $|ßNTI| < 2$, RC_{bray} index was defining to differentiate between the influence of dispersal limitation (above +0.95), homogenizing dispersal (below −0.95) or ecological drift (values ranging from −0.95 to 0.95; Stegen et al. 2013). Additionally, to quantify ecological stochasticity in community assembly, the modified stochasticity ratio (MST; Liang et al. 2020) was calculated using the NST package in R v.3.6.0. Values above the boundary point (50%) indicated that assembly was more stochastic and values < 50% more deterministic. Stochasticity ratio (ST; Zhou et al. 2014), standard effect size (SES; Kraft et al. 2011), and normalized stochasticity ratio (NST; Ning et al. 2019) were also measured to complement the hypotheses based on the different null model algorithms.

Results

Microcosms' chemical properties and methane yields

Microcosms were prepared using a salt saturated slurry collected from hypersaline anaerobic sediments (Font-Verdera et al. 2021) as inoculum, and the slurry was diluted to salinities ranging from 30% to 5% to obtain an optimal methanogenic production consortium and to analyze the influence of salinity concentration, ampicillin amendment, and *P. oceanica* leaf litter biomass during community assembly. Permutation *D*-test, Kolmogorov–Smirnov (with Bonferroni correction), and Wilcoxon (parameters: $D \leq 1.36$ and $P > 0.05$) and *T*-test ($\alpha = 0.05$ and $|t| \leq 1$; Table S1, Supporting Information) showed no statistically significant differences between the duplicated enrichments. Therefore, microcosms under the same conditions were considered as duplicates.

The concentrations of the major salts in the decreasing salinities (from 30% to 5% w/v) are given in Figure S2 (Supporting Information). Sodium chloride (NaCl) was the dominant salt and ranged from 3.7 M (in the microcosmos with 30% salinity and the original slurry) to 0.5 M (5% salinity). The same pattern was observed for the magnesium sulfate ($MgSO_4$: 0.5–0.05 M), magnesium chloride ($MgCl_2$: 0.35–0.1 M), and potassium chloride (KCl: 0.16–0.0 M). Conversely, calcium carbonate ($CaCO_3$) increased as salinity decreased (from 14 M at 5% of salinity to 0.5 M at 30%) while calcium chloride ($CaCl_2$) did not differ between salinities (0.0–0.03 M).

Methane concentration experienced an increment in the microcosms, especially during the first year (Figure S1, Supporting Information). The highest methane production was at 5% salinity, 10% of *P. oceanica* biomass and amended with ampicillin (5_10A), generating molarities as high as 782.2 mM after 3 years, nearly one order of magnitude higher than the average of maximum values displayed in other conditions (85.8 mM—~4 years). Below 15% of salinity, microcosms amended with antibiotic displayed higher methane concentrations, with an average of~290 mM and ~359 mM. On the other hand, salinities of ≥15% showed an opposite trend, where methanogenesis was moderate after 9 months, and overall the antibiotic supplementation caused a reduction in methane yields.

Changes in the microbial community structure in the salinity gradient

A total of 6 223 459 746 raw read were generated. After trimming and chimera removal, the dataset was rarified and after the phylogenetic inference rendered 1468 OPUs (For details, see 16S rRNA gene sequence processing in Table S2, Supporting Information).

Richness (Chao-1) values decreased as salinity increased (transitioning from a positive to negative change in relation to the inoculum, with its values of Chao-1 of 39 and 116, for archaea and bacteria, respectively), displaying bacteria highest index values (Fig. 1A and B). With few exceptions, Shannon index in archaea was overall lower in microcosms when compared to the inoculum ($H = 3.394$; Fig. 1C). Conversely, Shannon index in bacteria was generally higher than the inoculum ($H = 2.988$, Fig. 1D), especially at 5% of salinity (Fig. 1C and D; Table S3, Supporting Information). Dominance generally increased in archaea with dilution, being highest at 5%, and with the exception of 12% salinity where the index decreased with regard to the inoculum. The opposite was observed for bacteria, which displayed increased dominance at high salinities (Figures S3a, S3b, and Table S3, Supporting Information).

NMDS plots based on Bray–Curtis dissimilarity showed the sample grouping by salinity (Fig. 2; Figure S4, Supporting Information), and dissimilarity was highest within microcosms at 5% of salinity (from 0.6 to 0.93), observing statistically significant differences within communities at each salinity ($P < 0.05$, Wilcoxon and Mann–Whitney *U* nonparametric tests; Figure S5, Supporting Information). Dissimilarity decreased as salinity increased, being lowest at 30% (from 0.3 to 0.5) and similar to the inoculum (with a Bray–Curtis dissimilarity average of 0.4). Furthermore, the highest turnover in diversity was observed at 15% of salinity (those communities from 30% until those of 18% of salinity were more similar among them) and at 5% (being the microbial populations of 12% and 10% alike those of 15%; Figure S4, Supporting Information).

Aiming to identify characteristic OPUs of a specific salinity, microcosms at 30% saline were considered to resemble the original conditions of the community since no statistically significant differences were found with the inoculum community (Kolmogorov–Smirnov test and *t*-test; Table S4, Supporting Information). The number of OPUs with statistically significant differences (abs(log2 fold change) > 2 and *P*-value < 0.05) between the microcosms at the different salinities and 30% salinity increased as salinity decreased (Figure S6, Supporting Information), with nine OPUs being statistically more abundant at salinity 25%, increasing to 300 at 5% salinity.

Dominant species (≥ 5% relative sequence abundance) at each salinity, included OPUs affiliated to Unc. 20c-4, Unc. DHVEG-6, Unc. *Anaerolineaceae*, and Unc. *Desulfovermiculus* sp. at 5%, Unc. MSBL1 and Unc. *Marinilabiliaceae* at 10%–30% and Unc. *Halanaerobium* sp. and Unc. KTK 4A at salinity of 30%. No dominant OPU at the end of the experiment displayed a relative abundance higher than 5% in the inoculum (S; Table 1; Table ST3, Supporting Information).

Influence of ampicillin addition on the community structures

After 4.5 years, the amended ampicillin (5 mg/ml) exerted an effect on alpha diversity on end-assemblages studied here. We did not chemically measure the concentration of ampicillin at the

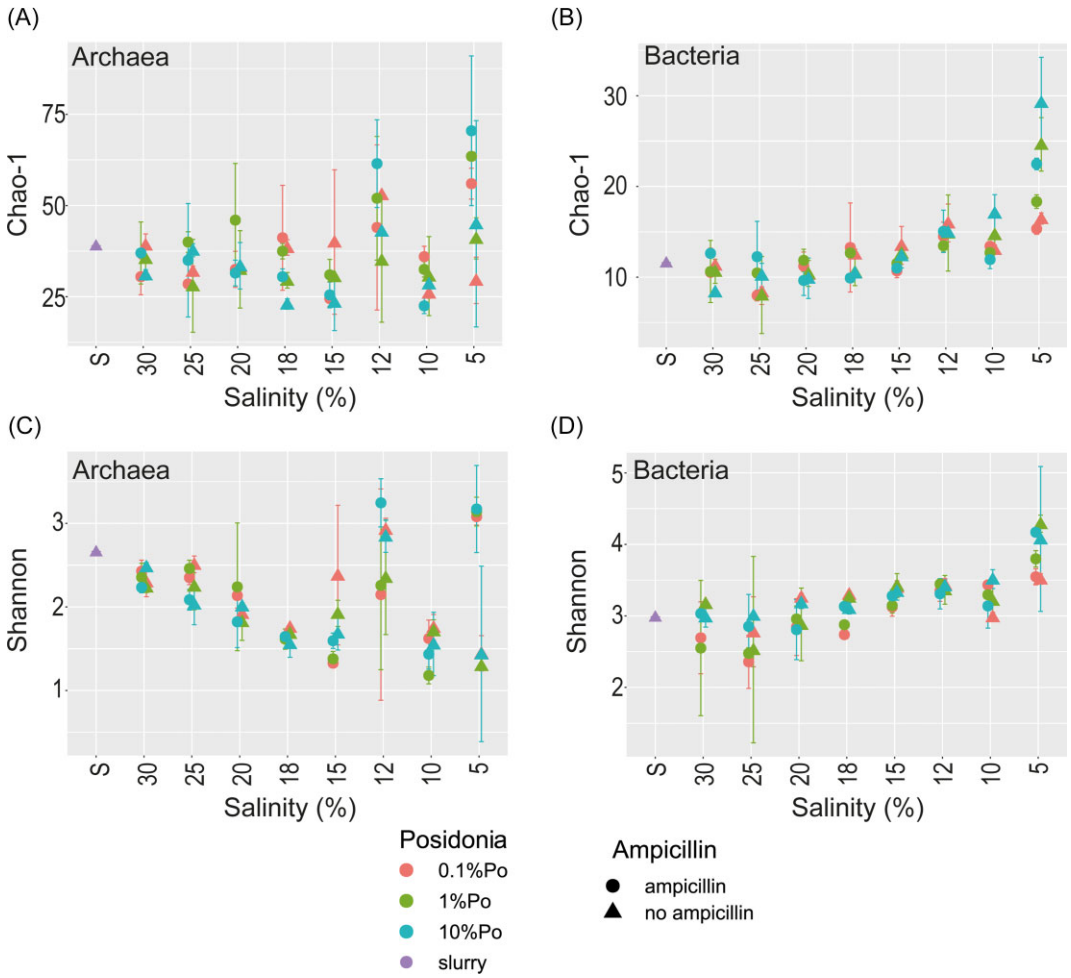

Figure 1. Diversity indices based on OPUs from 16S rRNA gene amplicons for archaeal (on the left) and bacterial (on the right) domains. Chao-1 (A) and (B) and Shannon (C) and (D) indices are shown according to the salinity, the ampicillin presence, and the *P. oceanica* substrate concentrations. Samples with concentrations of 0.1%, 1%, and 10% *Po* are colored in red, green, and blue, respectively. Samples with or without ampicillin are represented in circles or triangles, respectively. Slurry (in purple) and salinities are ordered from highest to lowest in the *x*-axes.

end of the experiment as we assumed that it would have been chemically or biologically degraded. At low salinities Chao-1 for archaea was higher in samples with ampicillin, increasing at 5% salinity in 80.8% with regard to the inoculum and only 35.9% without ampicillin. Bacteria displayed higher richness values at intermediate salinities (18%, 20%, and 25%) in the amended enrichments (Fig. 1A and B; Table S3, Supporting Information). Interestingly, Shannon index increased from 15.6% to 19.1% in microcosms with 5% salinity and ampicillin, being especially higher than those at the same salinity but without ampicillin (−45.7% to −51.2%; Fig. 1C and D; Table S3, Supporting Information). As observed in the NMDS, samples grouped by the presence/absence of the antibiotic (based on Bray–Curtis dissimilarity, Fig. 2) and at 5% salinity the effect of ampicillin was more notable. The communities assembled with or without amended antibiotic were statistically different (PCoA based in variance dispersion, Fig. 3A).

The addition of antibiotic promoted a statistically significant lower number of the dominant OPUs in comparison with the non-amended (Figure S6, Supporting Information). When ampicillin was added different species were not detected in different salinities. For example, *Sporosalibacterium* and *Brassicibacter* genera were not detected at 5% salinity (Table ST4, Supporting Information), or *Hydrogenedentes* at 10%–15% salinity and the Marine Benthic Group D and DHVEG-1 at 15%–18% salinity. The genus *Desulfovermiculus* and the family *Desulfobacteraceae* displayed lower abundances at salinities of 5%–12% and were not detected 15% and 30% salts. Some OPUs affiliated with the phylum *Acetothermia* displayed higher abundances with ampicillin at 5%–10% salinity, while others were not detected at 12%–15% salinity (Table ST4, Supporting Information). Additionally, some taxa were exclusively detected in the intermediate salinities such as of *Clostridiales* at 5%, uncultured *Bacteroidetes* at 15% and 20% salinity, and uncultured *Salinarchaeum*, MSBL1, and *Haloplasma contractile* at 18% of salts (Table ST5, Supporting Information).

Some taxa were detected with and without antibiotic but displayed higher abundances in the amended samples, such as members of the KTK 4A cluster at 5%–20% salinity, *Salinibacter* at 5%–15%, taxa affiliated to MSBL1 at all salinities but 10%, and *Christensenellaceae* R-7 group at 5%, 10%, and 12% salinities, among others (Table ST6, Supporting Information).

Influence of the *P. oceanica* leaf litter addition on the community structure

Overall, the concentration of *P. oceanica* as substrate did not substantially affect alpha diversity. Even if statistically significant differences were observed due to different substrate concentrations (permutation *D*-test: $D \leq 1.36$ and $P > 0.05$, and Wilcoxon:

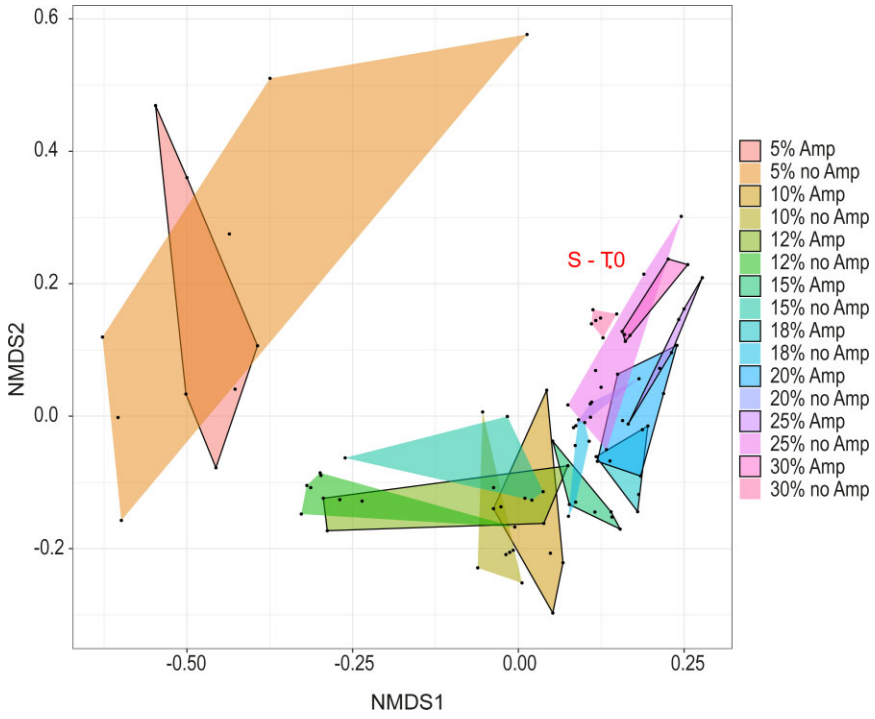

Figure 2. NMDS based on Bray–Curtis dissimilarity of 16S rRNA gene sequences from the 96 microcosms and the slurry sample (S—T0), marked in red. Samples are grouped according to the salinity and ampicillin in different colored polygons, which legend is on the right-side of the plot. Polygons with ampicillin are bordered and defined with "Amp," and without ampicillin with "noAmp."

$P \leq 0.5$; Table S5, Supporting Information), the effect of the antibiotic was overall more important (PCoA based in variance dispersion within groups, Fig. 3B). A high number of OPUs (reaching values of 85) was statistically significant of a single salinity and with a specific concentration of *P. oceanica* (abs(log2 fold change) > 2 and *P*-value < 0.05) and, although there were relevant OPUs detected at the three substrate concentrations as statistically significant, high differences in number of OPUs was always observed between the tested concentrations (Table ST7, Supporting Information).

Changes in the influence of ecological processes on community assembly caused by the salt dilution

In general, ßNTI values from pairwise comparisons between the inoculum and the microcosms showed a nondiscriminatory distribution, where no data exceeded the statistically significant boundary (|ßNTI| > 2). Overall, ßNTI in the archaea domain showed that the phylogenetic turnover was close to the null expectation, being the community mainly influenced by stochastic factors (Figures S12a and S12b, Supporting Information). The stochasticity decreased as salinity decreased since the replicates showed less dispersion in the index. In bacteria, the phylogenetic turnover was lower than in archaea as ßNTI was closer to −1, with the exception of 5% salinity where a higher phylogenetic turnover was observed, being ßNTI > 1 for some of the samples. As for archaea, and to a minor extent, the stochasticity seemed to increase with salinity in bacteria, as the dispersion between replicates increased with the exception of 5% salinity, where ßNTI of duplicates was also not reproducible (Figures S7a and S7b, Supporting Information). Raup–Crick metric based on Bray–Curtis dissimilarities (RC_{bray}) showed a fairly defined pattern with a descending trend as salinity increased (Fig. 4; Figures S7c and S7d, Supporting Information). Therefore, there was a transition in taxonomic turnover from low to high as samples were diluted and salinity decreased from the initial condition of salt saturation. According to this index, archaea was more influenced by stochasticity since, overall, RC_{bray} was closer to null expectation and the replicates were more dissimilar than in bacteria.

To quantify ecological stochasticity between the different conditions applied in microcosms, ST and NST ratios were calculated, displaying values > 55% and indicating the stochasticity dominance either in archaea or bacteria domains (Figures S8a and S8b, Supporting Information). The ST and NST ratios were above 70% and 60%. In archaea, NST ratio decreased with substrate concentration while the opposite was observed in bacteria (Figures S8c and S8d, Supporting Information). Furthermore, when we compared the ampicillin effect in relation to the inoculum, in general stochasticity decreased with salinity, ranging from 100% to 54%, excepting few samples with 5% and 12% salinity, which displayed values below the boundary of 50% in archaeal domain (Figure S8e, Supporting Information). MST exhibited a clear pattern of gradual transition of determinism dominance in the lowest salinities to stochasticity at those highest, denoting the differences between domains and especially among salinities (Figure S9a, Supporting Information). Accordingly, the SES, which measures the magnitude of the experimental effects, displayed increasing values as salinity decreased, being, therefore, at 5% of salinity where the effects of ampicillin were more relevant (Figure S9b, Supporting Information).

Dominant metabolic processes

Metabolic inferences were performed for species or OPUs with relative abundances ≥1% and related to carbohydrate degradation, fermentation, methanogenesis, chemolithoautotrophy, phototrophy, and sulfate- and nitrate-reduction (Table S6 and Figure S10, Supporting Information).

Table 1. Relevant OPUs from 16S rRNA gene sequences analyzed from the 96 microcosms and S, with relative abundances ≥ 5% (at least in one sample) for archaea (ARCH) and bacteria (BACT). First column (from left to right) is the OPU number, the following five columns show the taxonomic affiliation of the closest relative sequence used as reference (phylum, class, order, family, and genus/species, respectively). OPUs that are representatives of each salinity (statistically significant: abs(log2 fold change) > 2 and *P*-value < 0.05) are gray shaded in the last eight columns, ordered in decreasing salinities. Relative abundances data are shown in the spreadsheet Tables ST1 and ST2 (Supporting Information). Inferred metabolisms are indicated in the first column according to this color code: red—carbohydrates degrader, blue—fermenter, orange—methanogen, yellow—chemolithoautotroph, purple—phototroph, green—nitrate-reducer, and pink—sulfate-reducer. More details about metabolisms are displayed in Table S6 (Supporting Information). ∗Unc. = Uncultured species.

ARCH	phylum	class	order	family	genus - species	30%	25%	20%	18%	15%	12%	10%	5%
4	*Aenigmarchaeota*	-	-	-	Deep Sea Euryarchaeotic Group (DSEG)								
23	*Euryarchaeota*	-	-	-	Unc. KTK 4A								
25	*Euryarchaeota*	-	-	-	Unc. Marine Benthic Group D - DHVEG-1								
62	*Euryarchaeota*	*Halobacteria*	*Halobacteriales*	*Halobacteriaceae*	Unc. *Halobacteria* class								
136	*Euryarchaeota*	*Thermoplasmata*	*Thermoplasmatales*	-	Unc. 20c-4								
157	*Euryarchaeota i.s.*	-	-	-	Unc. MSBL1								
167	*Euryarchaeota i.s.*	-	-	-	Unc. MSBL1								
192	*Woesearchaeota*	-	-	-	Unc. DHVEG-6								
202	*Woesearchaeota*	-	-	-	Unc. DHVEG-6								
BACT	**phylum**	**class**	**order**	**family**	**genus - species**	**30%**	**25%**	**20%**	**18%**	**15%**	**12%**	**10%**	**5%**
18	-	-	-	-	Unc. TM6 (*Dependentiae*)								
24	-	-	-	-	Unc. WS1								
39	*Acetothermia*	-	-	-	Unc. *Acetothermia*								
156	*Bacteroidetes*	*Bacteroidia*	*Bacteroidales*	*Marinilabiliaceae*	Unc. *Marinilabiliaceae*								
157	*Bacteroidetes*	*Bacteroidia*	*Bacteroidales*	*Marinilabiliaceae*	Unc. *Marinilabiliaceae*								
165	*Bacteroidetes*	*Bacteroidia*	*Bacteroidales*	*Marinilabiliaceae*	Unc. *Marinilabiliaceae*								
276	*Chlamydiae*	*Chlamydiia*	*Chlamydiales*	*Simkaniaceae*	Unc. *Simkaniaceae*								
281	*Chlorobi*	*Chlorobia*	*Chlorobiales*	*Chlorobiaceae*	*Prosthecochloris vibrioformis*								
305	*Chloroflexi*	*Anaerolineae*	*Anaerolineales*	*Anaerolineaceae*	Unc. *Anaerolineaceae*								
318	*Chloroflexi*	*Anaerolineae*	*Anaerolineales*	*Anaerolineaceae*	Unc. *Anaerolineaceae*								
385	*Firmicutes*	*Bacilli*	*Bacillales*	*Bacillaceae*	*Halobacillus halophilus*								
386	*Firmicutes*	*Bacilli*	*Bacillales*	*Bacillaceae*	*Halobacillus mangrovi*								
409	*Firmicutes*	*Bacilli*	*Caryophanales*	*Bacillaceae*	*Paraliobacillus ryukyuensis*								
414	*Firmicutes*	*Bacilli*	*Caryophanales*	*Bacillaceae*	Unc. *Bacillus* sp.								
425	*Firmicutes*	*Bacilli*	*Caryophanales*	*Bacillaceae*	*Virgibacillus salarius*								
460	*Firmicutes*	*Clostridia*	*Eubacteriales*	-	Unc. MAT-CR-H4-C10								
469	*Firmicutes*	*Clostridia*	*Eubacteriales*	*Christensenellaceae*	Unc. *Christensenellaceae* R-7 group								
555	*Firmicutes*	*Clostridia*	*Halanaerobiales*	*Halanaerobiaceae*	Unc. *Halanaerobium* sp.								
559	*Firmicutes*	*Clostridia*	*Halanaerobiales*	*Halanaerobiaceae*	Unc. *Halanaerobium* sp.								
564	*Firmicutes*	*Clostridia*	*Halanaerobiales*	*Halanaerobiaceae*	Unc. *Halocella* sp.								
566	*Firmicutes*	*Clostridia*	*Halanaerobiales*	*Halanaerobiaceae*	Unc. *Halocella* sp.								
643	*Marinimicrobia*	-	-	-	Unc. SAR406 clade								
689	*Planctomycetes*	-	*Brocadiales*	*Brocadiaceae*	Unc. PB79								
1008	*Proteobacteria*	*Deltaproteobacteria*	*Desulfobacterales*	*Desulfobacteraceae*	Unc. *Desulfobacteraceae*								
1038	*Proteobacteria*	*Deltaproteobacteria*	*Desulfovibrionales*	*Desulfohalobiaceae*	Unc. *Desulfovermiculus* sp.								
1269	*Tenericutes*	*Mollicutes*	-	-	Unc. NB1-n								
1271	*Tenericutes*	*Mollicutes*	*Haloplasmatales*	*Haloplasmataceae*	*Haloplasma contractile*								

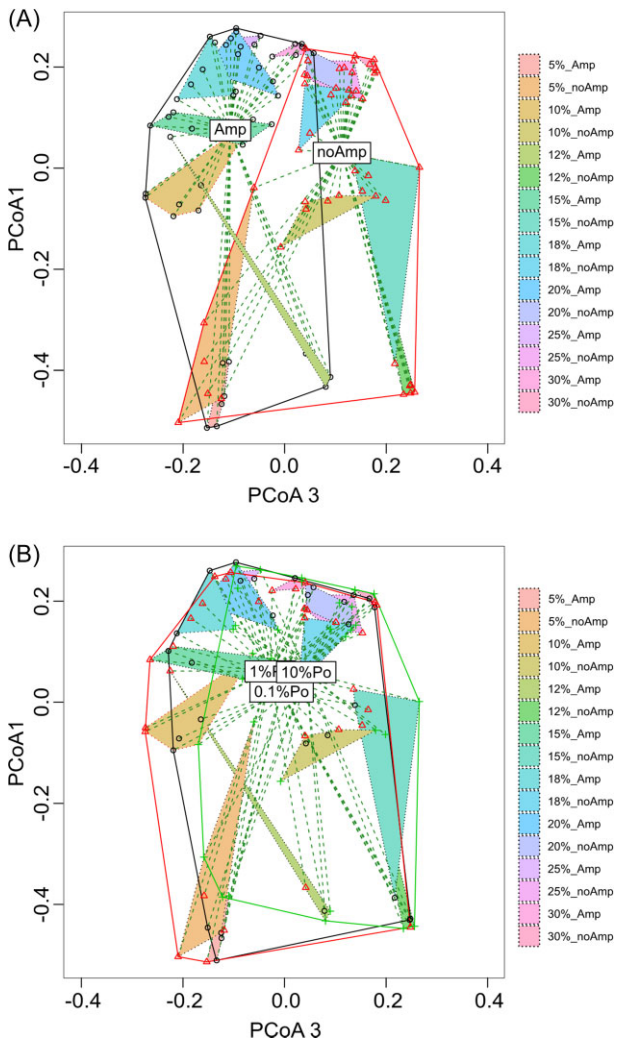

Figure 3. PCoA plots from analysis of multivariate homogeneity of groups dispersions (variances) applied to the 96 microcosms. (A) PCoA attending to samples with ampicillin (in black) and without the antibiotic (in red). (B) PCoA attending to the three substrate concentrations (0.1% *Po*, 1% *Po*, and 10% *Po*), grouped in black, red, and green colors.

The methanogenic representatives showed a distribution according to microcosms' salinities (Tables S1, S6, and Figure S10, Supporting Information). Taxa affiliated to MSBL1 were not present at 5% salinity, while at higher salinities, and especially in microcosms with low substrate concentrations and ampicillin, the members of this group showed high abundances. In general, methylotrophy was relevant in the lowest salinities (12%, 10%, and 5%) as the *Methylobacterium* genus was the main representative (Table S6, Figures S10c, S11c, and S11d, Supporting Information). Other methanogens were only present at 5% salinity, such as *Methanolacinia paynteri*, Unc. *Methanoculleus*, Unc. *Lokiarchaeota*, Unc. Marine Benthic Group D, or DHVEG-1. Acetogenic microorganisms, such as Unc. *Acetothermia*, were also relevant at low salinities.

Taxa described as carbohydrate degraders, showed contrasting trends in abundance, especially in microcosms at intermediate or higher salinities without ampicillin, such as the uncultured SAR406 group, uncultured KTK 4A and the *Halanaerobium* genus (Table S6, Figures S10b, S11a, S11f, and S11g, Supporting Information).

Chemolithoautotrophic *Acetothermia* phylum displayed higher richness in the intermediate salinities (from 12% to 20%) in samples amended with ampicillin and 10% w/w of substrate, although the different species within this phylum showed a turnover pattern (Table S6, Figures S10d, and S11e, Supporting Information). Chemoorganotrophy was detected by e.g. the presence of members of the *Marinilabiliaceae* and *Simkaniaceae* families, with the former being present at all salinities but 5% and the latter being only present at 5%. Overall, chemoorganotrophs displayed lower abundances in microcosms where the antibiotic was added. *Prosthecochloris vibrioformis* displayed relative abundances ~28% at 5% of salinity, 0.1% *Po* and without ampicillin, highlighting the presence of phototrophy in this specific setting (Table S6, Figures S10e, and S10f, Supporting Information). Furthermore, *H. contractile*, able to reduce nitrate and nitrite, was only present at salinities between 15% and 10% (Table S6 and Figure S10g, Supporting Information). Members of *Desulfobacteraceae* and the genus *Desulfovermiculus*, as the most representative sulfate- and sulfite-reducers, were present in microcosms with salinities below 20%, and especially abundant at 12% salinity, close to 25% in some samples (Table S6, Figures S10h, S11i, and S11j, Supporting Information).

Discussion

Salt dilution as major factor structuring the microbial community

Here, we could demonstrate that salinity acted as a major determinant factor on the community structuration of a diluted hypersaline slurry (~36% salts) in a broad gradient of decreasing ion concentrations and after ≥ 4 years of incubation. Although the main diversity originated from the source was conserved, a phylogenetic turnover was observed between microcosms at different salinities, and this selective role that has been reported before in solar salterns (Viver et al. 2019), saline soils (Xie et al. 2017), hypersaline sediments from lakes (Jiang et al. 2007), and hypersaline soda lakes (Vavourakis et al. 2018). As expected for a hypersaline adapted community, the progressive dilution of the slurry meant that the lowest salinity experimented the highest disturbance. Congruently, 5% salinity displayed the highest compositional changes regarding the inoculum. The dilution directly affected the alpha diversity by means of the higher sensitivity of archaea to osmotic changes (Viver et al. 2020) and the better adaptation of bacteria to low salinities (Ventosa and Arahal 2009). In turn, alpha diversity increased as salinity decreased. Almost all prokaryotes originated from the source hypersaline sediment, with the minor addition of the accompanying microorganisms from the *P. oceanica* litter, brines and seawater used to dilute the sediments. The cell numbers that may be inoculated from this leaf litter may be negligible as they are orders of magnitude lower than the original slurry 10^8 cells/ml (López-López et al. 2010). The community changes and detection of undetected taxa in the original sample would evidence the importance of the rare biosphere (including the low cellular addition from the substrate) in ecosystems with changing physicochemical conditions, which would act as a seed bank increasing in relative abundance when the conditions are favorable (Pedrós-Alió 2012).

Aiming to modulate the enrichments of methanogenic consortia (Sanz et al. 1996) for future biotechnological purposes, and to study the effect of a bacterial perturbing factor (Holmes and Smith 2016, Sela-Adler et al. 2017), ampicillin was added to a subset of the microcosms. To our knowledge, the study of antibiotic effects in hypersaline anoxic environments has never been

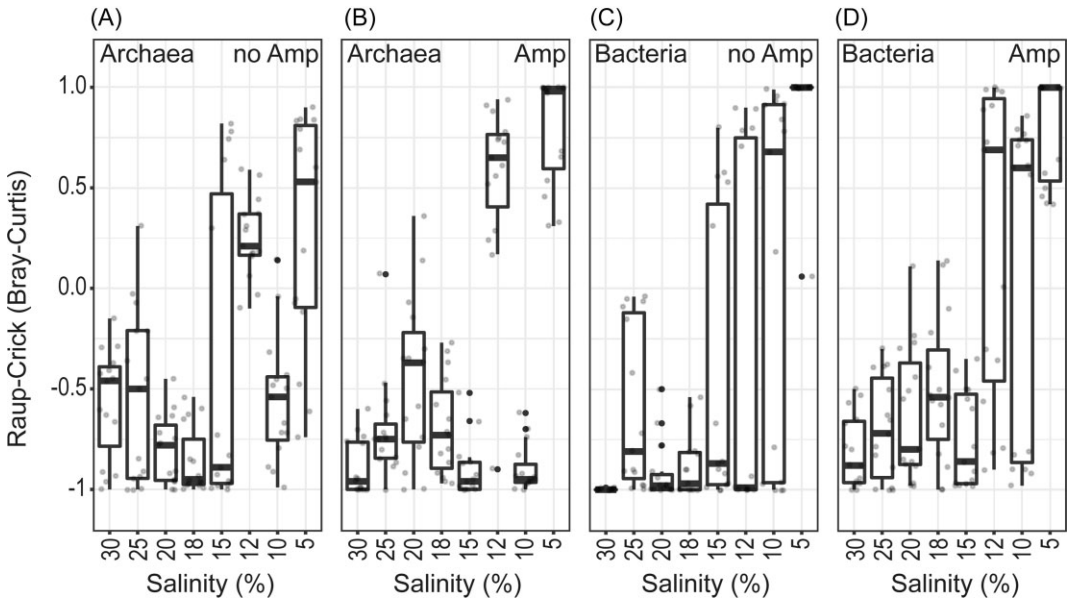

Figure 4. Raup–Crick data based on Bray–Curtis dissimilarity, calculated for all microcosms and classified by salinity depending on domain of microbial communities and the ampicillin addition. In the x-axes, from left to right, the samples are ordered in decreasing salinities, separated by domains (archaea in the left—A and B; and bacteria in the right—C and D) and within each domain, according to ampicillin presence (without antibiotic in the left—A and C; and with ampicillin in the right—B and D).

performed. Previous studies have assessed the effect of this antibiotic in other ecosystems such as soils, wastewater or freshwater (Ye et al. 2020), where ampicillin decreased the abundance of certain community members, hindering relevant ecosystem metabolic functions (Ferrer et al. 2017, Baumgartner et al. 2020, Ye et al. 2020). As expected, the addition of ampicillin at 5 mg/ml in microcosms reduced community bacterial alpha diversity at the long term (4.5 years). Beta diversity between with and without ampicillin displayed an increasing trend with dilution, although its real effect could be partially hidden by the salinity factor (Lauber et al. 2009, Rousk et al. 2010). The higher observed divergence between microcosms amended with antibiotic at lower salinities is related to the fact that ampicillin overall targets susceptible, usually Gram-positive bacteria, which are more abundant at lower salinities. Probably dissimilatory sulfate-reducing microorganisms were affected by the addition of ampicillin at the beginning of the experiment. In fact, at salinity of 5%, the relative abundances of sulfate-reducers (overall Gram-positives) decreased with ampicillin, while the uncultured MSBL9 cluster even seemed to disappear with the presence of the antibiotic, being statistically significant in cultures without the beta-lactam antibiotic (Table ST8, Supporting Information). Interestingly, archaeal alpha diversity at 5% salinity was higher in microcosms with ampicillin. This could be related to the emergence of new niches to be colonized due to the elimination of bacterial groups that are sensitive to the antibiotic, such as *Anaerolinea* and *Caldilinea* genera whose abundance decreased with ampicillin. As expected, members belonging to *Bacillota* phylum (formally *Firmicutes*) decreased their presence in cultures with ampicillin, being species statistically significant in samples without ampicillin at 15% of salinity (Table ST8, Supporting Information). Alternatively, the effect of carbon substrate concentration did not show an important effect on community diversity. This could be related with a low reactivity of the *Posidonia* litter that seems to be recalcitrant (Medina et al. 2001) to make carbon available to fermenters. Although some effect was observed by the substrate concentration on the community structure, it was weak and might be linked to immigrant microbial populations present in the litter reinforcing that the major changes came from the autochthonous microbial communities in the sediments.

Determinism became relevant with dilution

In general, both phylogenetic and taxonomic turnover was low and overall, not different from the null expectation, thus indicating that stochasticity generally prevailed. Salinity was the major ecological factor involved in the community assembly, being higher the stochasticity and lower the effect size in the higher salinities. The original community belonged to a highly adapted microbiome to hypersaline and anaerobic conditions. In such ecological state, selection eventually had led to a stable community with low turnover where drift became the most relevant factor (Stegen et al. 2012, Liébana et al. 2019). Archaea was more affected by stochasticity than bacteria due to the dominance of the former at higher salinities. Dilution exerted a selection of the community members able to thrive at lower salinities (Langenheder et al. 2017). Turnover between replicates decreased as salinity decreased, revealing determinism to gain relevance with dilution. Moreover, the importance of the ampicillin amendment was also observed, exerting slightly different effects in the archaeal and bacterial communities. Salinity acted as a selection force and ampicillin applied a selective pressure that changed the structure of microbial populations, consistent with other studies (Ye et al. 2020). The manipulation of natural ecosystems applying a dilution gradient has its drawbacks. The loss of rare taxa and the overrepresentation of others influence the taxonomic structure and the metabolic processes associated to them (Sierocinski et al. 2018).

Biogeochemical changes in microcosms were mainly driven by salinity dilution

The most abundant OPUs affiliated with microorganisms were putatively involved in methanogenesis (e.g. MSBL1, *M. paynteri*, and *Methanoculleus* genus) and sulfate-reduction (e.g. *Desulfatiglans*, *Desulfovermiculus*, *Desulfobulbus*, and *Sulfobacillus* genera). These metabolic groups displayed, generally, an opposite relative abundance pattern, with sulfate-reducers decreasing and

methanogens increasing as salt concentration did. Interestingly, there was a replacement of methanogens by sulfate-reducers at 12% salinity, it seems that sulfate-reducers might outcompete methanogens and display an optimum growth at 10%–12%, being strongly inhibited at 21.5%, which together with the reported inhibition of methanogens by sulfate-reduction at salinities below 18% might explain the observed replacement of these communities at 12% of salinity (Sørensen et al. 2004). This is also supported by the unexpected and higher methane production yield observed in microcosms with low salinities where ampicillin was added. In general, methane production was highest at 18%–20% salinities, with the exception of microcosm 5_10A that showed the highest yields. At higher salinities, the putative methanogens affiliated to MSBL1 dominated, and seemed to be the main responsible in the methane generation. We have previously reported the potential methanogenic activity of MSBL1 in hypersaline conditions (Font-Verdera et al. 2021). Here, at these intermediate salinities, where sulfate reducers were not competing for substrates and a likely higher concentration of methylamines derived from compatible solutes, such as glycine betaine, produced by halophiles, would have enhanced the methylotrophic methanogenesis (McGenity and Sorokin 2019).

It should be noted that the methane concentrations here obtained were remarkably higher when compared to the retrieved methane rates in previous studies of hypersaline sediments and slurries at low salinity (Sørensen et al. 2004, Mcgenity 2010, Lazar et al. 2011, Gründger et al. 2015, Webster et al. 2015, Nigro et al. 2020). The metabolic efficiency has been reported elsewhere to decrease up to 50% due to the loss of half of the rare fraction of the community (Sierocinski et al. 2018). In our case, this fact could be compatible with the disturbance caused here that could have caused the loss of rare and low abundant taxa if sensitive to osmotic changes, and consequently, the overrepresentation of the abundant taxa.

Finally, we found that the microcosms at 5%, where the highest dilution was applied, to be the most efficient in terms of methane production. This could be related to inhibition of methanogenesis caused by salinity. Zhang et al. (2017) reported the methanogenesis to be hindered at salinities greater than 5.5%, especially some hydrogenotrophic and aceticlastic methanogens. Here, we did not observe such phenomenon as we obtained a high methane yield production at salinities between 20% and 18%. In this regard, slurry experiments from a microbial mat in a saltern pond in Eilat revealed high methane production rates only between 15% and 25% of salinity (Sørensen et al. 2004). Conspicuously, the microcosms at 5% of salinity amended with ampicillin and substrate at 10% showed the highest methane rate, observed in both replicates. The conditions applied in these microcosms appears to have selected an efficient methanogen community, where the antibiotic may be the influencing selecting factor. This community was not remarkably different from others found in microcosms amended at 5% salinities, yet the differences were enough to obtain methane yields up to 12 times higher compared to previously detected at similar salinities (Sørensen et al. 2004, Mcgenity 2010, Lazar et al. 2011, Gründger et al. 2015, Webster et al. 2015, Nigro et al. 2020). These high rates of methanogenesis in hypersaline sediments demonstrates the potential of these still unexplored environments. These observations may be relevant in the context of methane production using saline water with salt concentrations above any marine waters, and explore possible applications of high biotechnological interests as it is our intention with the consortium at 5% of salinity amended with antibiotic and with 10% of *P. oceanica*.

Sampling permits

The samples were taken in accordance with the permit ESNC27, with the unique identifier ABSCH-IRCC-ES-241224–1 that has been provided by the Dirección General de Biodiversidad y Calidad Ambiental del Ministerio para la Transición Ecológica of the Spanish Government.

Authors' contributions

Francisca Font-Verdera, Raquel Liébana, Ramon Rossello-Mora, and Tomeu Viver.

Acknowledgments

The authors would like to thank all those responsible of Salinas S'Avall (Colònia de Sant Jordi, Mallorca, Spain) for the admittance to their installations and sampling permission.

Supplementary data

Supplementary data is available at *FEMSEC Journal* online.

Conflict of interest: The authors declare that there is no conflict of interest. All samples of this study were taken before the Spanish Real Decreto 124/2017 that rules the access to natural samples without commercial purposes.

Funding

This work was supported by the Spanish Ministry of Science, Innovation and Universities projects PGC2018-096956-B-C41, RTC-2017-6405-1, and PID2021-126114NB-C42, which were also supported with European Regional Development Fund (FEDER) funds. R.R.M. acknowledges the researcher mobility (grant numbers PRX18/00048 and PRX21/00043), F.F.V.'s the fellowship (grant number BES-2016-078138), and T,V, the "Margarita Salas" postdoctoral grant, all funded by the Spanish Ministry of Science, Innovation and Universities, and also within the framework of Recovery, Transformation and Resilience Plan, and funded by the European Union (NextGenerationEU), with the participation of the University of Balearic Islands (UIB). This research was carried out within the framework of the activities of the Spanish Government through the "Maria de Maeztu Centre of Excellence" accreditation to IMEDEA (CSIC-UIB) (CEX2021-001198).

Data availability

Some of the data that support the findings of this study are available in the supplementary material of this article, in the online version. The experimental data, collection of samples, and analyses have been only used by the first author of the manuscript to prepare her PhD thesis document i.e. available at the repository of University of Balearic Islands (https://dspace.uib.es/xmlui/bitstream/handle/11201/159809/Francesca%20Font%20Verdera_TESIS%20DEF.pdf?sequence=1&isAllowed=y).

References

Antón J, Rosselló-Mora R, Rodríguez-Valera F *et al.* Extremely halophilic bacteria in crystallizer ponds from solar Salterns. *Appl Environ Microbiol* 2000;**66**:3052–7.

Baumgartner M, Bayer F, Pfrunder-Cardozo KR *et al.* Resident microbial communities inhibit growth and antibiotic-resistance evolu-

tion of *Escherichia coli* in human gut microbiome samples. *PLoS Biol* 2020;**18**:1–30.
Callahan BJ, McMurdie PJ, Rosen MJ *et al.* DADA2: high resolution sample inference from Illumina amplicon data. *Nat Methods* 2016;**13**:581–92.
Caporaso JG, Lauber CL, Walters WA *et al.* Global patterns of 16S rRNA diversity at a depth of millions of sequences per sample. *Proc Natl Acad Sci USA* 2011;**108**:4516–22.
Chase JM, Kraft NJB, Smith KG *et al.* Using null models to disentangle variation in community dissimilarity from variation in α-diversity. *Ecosphere* 2011;**2**:1–11.
Cheng L, Wu K, Zhou L *et al.* Isolation of a methyl-reducing methanogen outside the euryarchaeota. *Biol Sci* 2023;**21**:1–26.
Cocozza C, Parente A, Zaccone C *et al.* Comparative management of offshore *Posidonia* residues: composting vs. energy recovery. *Waste Manag* 2011;**31**:78–84.
Dębowski M, Zieliński M, Grala A *et al.* Algae biomass as an alternative substrate in biogas production technologies – review. *Renew Sustain Energy Rev* 2013;**27**:596–604.
Dini-Andreote F, Stegen JC, Van Elsas JD *et al.* Disentangling mechanisms that mediate the balance between stochastic and deterministic processes in microbial succession. *Proc Natl Acad Sci USA* 2015;**112**:E1326–32.
Ferrer M, Méndez-García C, Rojo D *et al.* Antibiotic use and microbiome function. *Biochem Pharmacol* 2017;**134**:114–26.
Font-Verdera F, Liébana R, Aldeguer-Riquelme B *et al.* Inverted microbial community stratification and spatial–temporal stability in hypersaline anaerobic sediments from the S'Avall solar salterns. *Syst Appl Microbiol* 2021;**44**:126231.
França L, Lopéz-Lopéz A, Rosselló-Móra R *et al.* Microbial diversity and dynamics of a groundwater and a still bottled natural mineral water. *Environ Microbiol* 2015;**17**:577–93.
Gomariz M, Martínez-García M, Santos F *et al.* From community approaches to single-cell genomics: the discovery of ubiquitous hyperhalophilic bacteroidetes generalists. *ISME J* 2015;**9**:16–31.
Gottschalk G. *Bacterial metabolism*. In: *Microbiology S series*. 1st edn., New York: Springer-Verlag, 1979, c1979.
Gründger F, Jiménez N, Thielemann T *et al.* Microbial methane formation in deep aquifers of a coal-bearing sedimentary basin, Germany. *Front Microbiol* 2015;**6**:1–17.
Hammer Ø, Harper DAT, Ryan PD. PAST: paleontological statistics software package for education and data analysis. *Palaeontol Electrónica* 2001;**4**:1–9.
Hatzenpichler R, Kohtz A, Krukenberg V *et al.* Cultivation and visualization of a methanogen of the phylum thermoproteota. *Biol Sci* 2023;**12**:1–22.
Holmes DE, Smith JA. Biologically produced methane as a renewable energy source. *Adv Appl Microbiol* 2016;**97**:1–61.
Jiang H, Dong H, Yu B *et al.* Microbial response to salinity change in Lake Chaka, a hypersaline lake on Tibetan plateau. *Environ Microbiol* 2007;**9**:2603–21.
Kraft NJB, Comita LS, Chase JM *et al.* Disentangling the drivers of β diversity along latitudinal and elevational gradients. *Science* 2011;**333**:1755–8.
Langenheder S, Wang J, Karjalainen SM *et al.* Bacterial metacommunity organization in a highly connected aquatic system. *FEMS Microbiol Ecol* 2017;**93**:1–9.
Lauber CL, Hamady M, Knight R *et al.* Pyrosequencing-based assessment of soil pH as a predictor of soil bacterial community structure at the continental scale. *Appl Environ Microbiol* 2009;**75**:5111–20.
Lazar CS, Parkes RJ, Cragg BA *et al.* Methanogenic diversity and activity in hypersaline sediments of the centre of the Napoli mud volcano, Eastern Mediterranean Sea. *Environ Microbiol* 2011;**13**:2078–91.
Liang Y, Ning D, Lu Z *et al.* Century long fertilization reduces stochasticity controlling grassland microbial community succession. *Soil Biol Biochem* 2020;**151**:108023.
Liébana R, Modin O, Persson F *et al.* Combined deterministic and stochastic processes control microbial succession in replicate granular biofilm reactors. *Environ Sci Technol* 2019;**53**:4912–21.
López-López A, Richter M, Peña A *et al.* New insights into the archaeal diversity of a hypersaline microbial mat obtained by a metagenomic approach. *Syst Appl Microbiol* 2013;**36**:205–14.
López-López A, Yarza P, Richter M *et al.* Extremely halophilic microbial communities in anaerobic sediments from a solar Saltern. *Environ Microbiol Rep* 2010;**2**:258–71.
Lozupone CA, Knight R. Global patterns in bacterial diversity. *Proc Natl Acad Sci USA* 2007;**104**:11436–40.
Ludwig W, Strunk O, Westram R *et al.* ARB: a software environment for sequence data. *Nucleic Acids Res* 2004;**32**:1363–71.
Martin-Cuadrado AB, Senel E, Martínez-García M *et al.* Prokaryotic and viral community of the sulfate-rich crust from Peñahueca ephemeral lake, an astrobiology analogue. *Environ Microbiol* 2019;**21**:3577–600.
McGenity TJ, Oren A. Hypersaline environments. In: Bell EM (ed.), *Life at Extremes: Environments. Organisms and Strategies for Survival*. Wallingford: CABI, 2012, 402–37.
McGenity TJ, Sorokin DY. Methanogens and methanogenesis in hypersaline environments. In:AJMStams,DZSousa (eds), *Biogenesis of Hydrocarbons, Handbook of Hydrocarbon and Lipid Microbiology*. Cham: Springer, 2019, 283–309.
Mcgenity TJ. Chapter 53 - methanogens and methanogenesis in hypersaline environments. In: *Handbook of Hydrocarbon and Lipid Microbiology*. **Vol. 1**. Berlin: Springer-Verlag, 2010, 665–80.
Medina JR, Tintoré J, Duarte CM. Las praderas de *Posidonia oceanica* y la regeneración de playas. *Rev Obras Publicas* 2001;**148**:31–43.
Mora-Ruiz MdR, Cifuentes A, Font-Verdera F *et al.* Biogeographical patterns of bacterial and archaeal communities from distant hypersaline environments. *Syst Appl Microbiol* 2018;**41**:139–50.
Mora-Ruiz MdR, Font-Verdera F, Díaz-Gil C *et al.* Moderate halophilic bacteria colonizing the phylloplane of halophytes of the subfamily *Salicornioideae* (*Amaranthaceae*). *Syst Appl Microbiol* 2015;**38**:406–16.
Mora-Ruiz MDR, Font-Verdera F, Orfila A *et al.* Endophytic microbial diversity of the halophyte arthrocnemum macrostachyum across plant compartments. *FEMS Microbiol Ecol* 2016;**92**:1–10.
Munoz R, López-López A, Urdiain M *et al.* Evaluation of matrix-assisted laser desorption ionization-time of flight whole cell profiles for assessing the cultivable diversity of aerobic and moderately halophilic prokaryotes thriving in solar Saltern sediments. *Syst Appl Microbiol* 2011;**34**:69–75.
Nigro LM, Elling FJ, Hinrichs KU *et al.* Microbial ecology and biogeochemistry of hypersaline sediments in Orca Basin. *PLoS ONE* 2020;**15**:1–25.
Ning D, Deng Y, Tiedje JM *et al.* A general framework for quantitatively assessing ecological stochasticity. *Proc Natl Acad Sci USA* 2019;**116**:16892–8.
Oksanen AJ, Blanchet FG, Friendly M *et al.* Vegan: community ecology package. R package version 2.4-4. CRAN, 2018 , 298.
Oren A. Microbial life at high salt concentrations: phylogenetic and metabolic diversity. *Saline Syst* 2008;**4**:1–13.
Pedrós-Alió C. The rare bacterial biosphere. *Ann Rev Mar Sci* 2012;**4**:449–66.

Pruesse E, Peplies J, Glöckner FO. SINA: accurate high-throughput multiple sequence alignment of ribosomal RNA genes. *Bioinformatics* 2012;**28**:1823–9.

Ramos-Barbero MD, Martin-Cuadrado AB, Viver T *et al.* Recovering microbial genomes from metagenomes in hypersaline environments: the good, the bad and the ugly. *Syst Appl Microbiol* 2019;**42**:30–40.

Rodriguez-R LM, Gunturu S, Tiedje JM *et al.* Nonpareil 3: fast estimation of metagenomic coverage and sequence diversity. *mSystems* 2018;**3**:1–9.

Rodriguez-R LM, Konstantinidis KT. Nonpareil: a redundancy-based approach to assess the level of coverage in metagenomic datasets. *Bioinformatics* 2014;**30**:629–35.

Rousk J, Bååth E, Brookes PC *et al.* Soil bacterial and fungal communities across a pH gradient in an arable soil. *ISME J* 2010;**4**:1340–51.

Santos F, Yarza P, Parro V *et al.* Culture-independent approaches for studying viruses from hypersaline environments. *Appl Environ Microbiol* 2012;**78**:1635–43.

Sanz JL, Rodríguez N, Amils R. The action of antibiotics on the anaerobic digestion process. *Appl Microbiol Biotechnol* 1996;**46**:587–92.

Sela-Adler M, Ronen Z, Herut B *et al.* Co-existence of methanogenesis and sulfate reduction with common substrates in sulfate-rich estuarine sediments. *Front Microbiol* 2017;**8**:1–11.

Serrano-Silva N, Sarria-Guzmán Y, Dendooven L *et al.* Methanogenesis and methanotrophy in soil: a review. *Pedosphere* 2014;**24**:291–307.

Sierocinski P, Bayer F, Yvon-Durocher G *et al.* Biodiversity–function relationships in methanogenic communities. *Mol Ecol* 2018;**27**:4641–51.

Sørensen KB, Canfield DE, Oren A. Salinity responses of benthic microbial communities in a solar saltern (Eilat, Israel). *Appl Environ Microbiol* 2004;**70**:1608–16.

Sorokin DY, Makarova KS, Abbas B *et al.* Discovery of extremely halophilic, methyl-reducing euryarchaea provides insights into the evolutionary origin of methanogenesis. *Nat Microbiol* 2017a;**2**:1–11.

Sorokin DY, Messina E, Smedile F *et al.* Discovery of anaerobic lithoheterotrophic haloarchaea, ubiquitous in hypersaline habitats. *ISME J* 2017b;**11**:1245–60.

Stegen JC, Lin X, Fredrickson JK *et al.* Quantifying community assembly processes and identifying features that impose them. *ISME J* 2013;**7**:2069–79.

Stegen JC, Lin X, Konopka AE *et al.* Stochastic and deterministic assembly processes in subsurface microbial communities. *ISME J* 2012;**6**:1653–64.

Swan BK, Ehrhardt CJ, Reifel KM *et al.* Archaeal and bacterial communities respond differently to environmental gradients in anoxic sediments of a California hypersaline lake, the Salton Sea. *Appl Environ Microbiol* 2010;**76**:757–68.

van der Wielen PW, Bolhuis H, Borin S *et al.* The enigma of prokaryotic life in deep hypersaline anoxic basins. *Science* 2005;**307**:121–3.

Vass M. Bound to the past: historical contingency in aquatic microbial metacommunities. Digital Comprehensive Summaries of Uppsala Dissertations from the Faculty of Science and Technology 1887. Uppsala Universitet, 2020.

Vavourakis CD, Andrei AS, Mehrshad M *et al.* A metagenomics roadmap to the uncultured genome diversity in hypersaline soda lake sediments. *Microbiome* 2018;**6**:168–85.

Ventosa A, Arahal DR. Physico-chemical characteristics of hypersaline environments and their biodiversity. *Extremophiles*. 2009;**II**:16.

Viver T, Conrad RE, Orellana LH *et al.* Distinct ecotypes within a natural haloarchaeal population enable adaptation to changing environmental conditions without causing population sweeps. *ISME J* 2020;**15**:1178–91.

Viver T, Orellana LH, Díaz S *et al.* Predominance of deterministic microbial community dynamics in Salterns exposed to different light intensities. *Environ Microbiol* 2019;**21**:4300–15.

Viver T, Orellana LH, Hatt JK *et al.* The low diverse gastric microbiome of the jellyfish *Cotylorhiza tuberculata* is dominated by four novel taxa. *Environ Microbiol* 2017;**19**:3039–58.

Walsh DA, Papke RT, Doolittle WF. Archaeal diversity along a soil salinity gradient prone to disturbance. *Environ Microbiol* 2005;**7**:1655–66.

Wang C, Huang Y, Zhang Z *et al.* Salinity effect on the metabolic pathway and microbial function in phenanthrene degradation by a halophilic consortium. *AMB Exp* 2018;**8**:1–11.

Webster G, O'Sullivan LA, Meng Y *et al.* Archaeal community diversity and abundance changes along a natural salinity gradient in estuarine sediments. *FEMS Microbiol Ecol* 2015;**91**:1–18.

Xie K, Deng Y, Zhang S *et al.* Prokaryotic community distribution along an ecological gradient of salinity in surface and subsurface saline soils. *Sci Rep* 2017;**7**:1–10.

Yakimov MM, La Cono V, Slepak VZ *et al.* Microbial life in the Lake Medee, the largest deep-sea salt-saturated formation. *Sci Rep* 2013;**3**:1–9.

Yakimov MM, La Cono V, Spada GL *et al.* Microbial community of the deep-sea brine Lake Kryos seawater-brine interface is active below the chaotropicity limit of life as revealed by recovery of mRNA. *Environ Microbiol* 2015;**17**:364–82.

Yarza P, Ludwig W, Euzéby J *et al.* Update of the all-species living tree project based on 16S and 23S rRNA sequence analyses. *Syst Appl Microbiol* 2010;**33**:291–9.

Ye MQ, Chen GJ, Du ZJ. Effects of antibiotics on the bacterial community, metabolic functions and antibiotic resistance genes in mariculture sediments during enrichment culturing. *J Mar Sci Eng* 2020;**8**:1–26.

Zhang Y, Alam MA, Kong X *et al.* Effect of salinity on the microbial community and performance on anaerobic digestion of marine macroalgae. *J Chem Technol Biotechnol* 2017;**92**:2392–9.

Zhou J, Deng Y, Zhang P *et al.* Stochasticity, succession, and environmental perturbations in a fluidic ecosystem. *Proc Natl Acad Sci USA* 2014;**111**:E836–45.

Zhuang GC, Elling FJ, Nigro LM *et al.* Multiple evidence for methylotrophic methanogenesis as the dominant methanogenic pathway in hypersaline sediments from the Orca Basin, Gulf of Mexico. *Geochim Cosmochim Acta* 2016;**187**:1–20.

Received 27 April 2023; **revised** 2 October 2023; **accepted** 20 November 2023